China Ocean Eng., Vol. 27, No. 5, pp. 683– 692

DOI 10.1007/s13344-013-0057-1, ISSN 0890-5487

A Finite Element Cable Model and Its Applications Based on the Cubic Spline Curve*

FANG Zi-fan (方子帆)[1], HE Qing-song (贺青松), XIANG Bing-fei (向兵飞),
XIAO Hua-pan (肖化攀), HE Kong-de (何孔德) and DU Yi-xian (杜义贤)

College of Mechanical & Material Engineering, China Three Gorges University, Yichang 443002, China

(Received 19 March 2012; received revised form 8 October 2012; accepted 6 December 2012)

ABSTRACT

For accurate prediction of the deformation of cable in the towed system, a new finite element model is presented that provides a representation of both the bending and torsional effects. In this paper, the cubic spline interpolation function is applied as the trial solution. By using a weighted residual approach, the discretized motion equations for the new finite element model are developed. The model is calculated with the computation program complier by Matlab. Several numerical examples are presented to illustrate the numerical schemes. The results of numerical simulation are stable and valid, and consistent with the mechanical properties of the cable. The model can be applied to kinematics analysis and the design of ocean cable, such as mooring lines, towing, and ROV umbilical cables.

Key words: *tension stiffness*; *bending stiffness*; *torsion stiffness*; *cubic spline curve*; *Galerkin criterion*; *finite element model*

1. Introduction

The towed system is widely applied to the fields of data collection with ocean hydrology, deep sea mining, and anti-submarine warfare, and it consists of support vessel, towed cable, towing equipment and so on. The work efficiency and operation stability are improved distinctly by predicting the motion response of drag system. The stress of the cable may be small, even zero or negative in the low speed, and thus the bending stiffness and torsion stiffness will become the main factors of cable motion. The motion performance and response cause great difference compared with the normal speed. The motion of towed system in the low stress state is studied, which has an important guiding significance for further controlling the motion of towed system.

Ablow and Schechter (1983) developed a three-dimensional algorithm that includes inertial forces and discretized the problem in both space and time using a finite difference method. Triantafyllou (1984) and Dowling (1988) showed that it is essential to introduce the bending stiffness of the cable near zero tension points. Howell (1991) and Burgess (1992) developed a finite difference method for solving low-tension cable problems in consideration of bending stiffness in the governing equation and proved that the method is stable regardless of the cable tension magnitude. Grosenbaugh

* This work was financially supported by the Natural Science Foundation of Hubei Province of China (Grant No. 2010CDB10804).
1 Corresponding author. E-mail: fzf@ctgu.edu.cn

et al. (1993) and Banerjee and Do (1994) respectively proposed a numerical technique for calculating the two-dimensional and three-dimensional motions of a tethered underwater vehicle, which can simulate accurately the dynamics of cables that are under low tensions. Sun *et al.* (1994) developed an algorithm to predict the transient response of a system of serially connected cables and bodies during unsteady deployment from a surface vessel. Park *et al.* (2003) presented a numerical and experimental investigation into the dynamic behavior of a towed low tension cable applicable to a towed array sonar system for detecting submarines, in which an implicit finite difference algorithm is employed for solving the three-dimensional cable equations. Buckham *et al.* (2004) showed an efficient and novel third-order finite element method that provides a representation of both the bending and torsional effects and accelerates the convergence of the model at relatively large element sizes. Zhu *et al.* (2006) established the nonlinear towing system dynamic model of the towing ship and the towed ship connected with a cable based on the equations governing the motion of the ship and three-dimensional equations of the towed cable system. Zhu *et al.* (2008) discussed the principle of a strong nonlinear coupling movement among the support ship, umbilical tether, cage, and vehicle. Afterwards, he modeled the strong nonlinear hydrodynamics performances on underwater remotely operated vehicle including the umbilical cable (Zhu *et al.*, 2010). Fang *et al.* (2012) published a new finite element computer program to accurately calculate the deformation of cable in the towed system in consideration of the bending and torsional effects.

In this paper, the 3-D nonlinear motion equation of a cable is modeled by using the spline interpolation functions to simulate the cable element curve and considering the nonlinearity of cable based on the theory of slender rods, and the cable motion is simulated by programs in the Matlab.

2. Equations of Motion

To model the cable easily, we define an inertial reference frame (*X, Y, Z*), and a local coordinate systems (***t***, ***n***, ***b***) for cables with reference to Fig. 1, which illustrates the towed system, where *X* and *Y* point in perpendicular, and *Z* is aligned with gravity. The ***n*** axis is normal, ***b*** axis is bi-normal, ***t*** axis is tangent to the element pointing in the direction of increasing tether length. The transform between the local coordinate and inertial frames, ***D***, is formed from a set of Euler angles $Z-Y'-X''(\psi, \theta, \xi)$. These successive rotations bring the inertial *Z*-axis into alignment with the tangent direction of the cable segment, and the orientation of the *n* and *b* axes is constrained by setting one of the Euler angles, the initial ψ rotation about the inertial *Z*-direction, to zero. Thus,

$$\boldsymbol{D}=\begin{bmatrix} \cos\theta & -\sin\theta & 0 \\ \cos\xi\sin\theta & \cos\xi\cos\theta & \sin\xi \\ -\sin\theta\sin\xi & -\sin\xi\cos\theta & \cos\xi \end{bmatrix}, \tag{1}$$

where θ and ξ can be considered as traditional pitch and roll of the cable.

The changing orientation of the Frenet frame is quantified by two parameters: the curvature, *k*, and the torsion, γ. The base unit vectors are defined as:

$$\boldsymbol{t}=\boldsymbol{r}',\ \ \boldsymbol{n}=\boldsymbol{r}''/k,\ \ \boldsymbol{b}=\boldsymbol{r}'\times\boldsymbol{r}''/k \tag{2}$$

The curvature, k, defines the bend of the cable within an osculating plane that is formed by $\boldsymbol{t}$ and $\boldsymbol{n}$ at the point considered. Both k and γ are defined in terms of the spatial derivatives of the space curve:

$$k = (\boldsymbol{r}'' \cdot \boldsymbol{r}'')^{1/2}, \quad \gamma = \frac{\boldsymbol{r}' \cdot (\boldsymbol{r}'' \times \boldsymbol{r}''')}{\boldsymbol{r}'' \cdot \boldsymbol{r}''}. \tag{3}$$

To create a numerical model that includes the desired bending and torsion effects, it is necessary to derive the dynamics equations for a continuous tether, considering the tortuous profile that a tether forms in three-dimensional space. In existing literature, the cable is modeled as a slender flexible rod that sustains environmental, gravitational, and buoyancy forces.

The centerline of the cable in the deformed state is a space curve $r(s, t)$, as illustrated in Fig. 1. The space curve is defined by the position vector $\boldsymbol{r}$ which is a function of arc-length s (measured along the curve) and time t.

A cable segment is analyzed, as shown in Fig. 2. If the outward normal vector at the point of P and P' is consistent with the direction of arc length increasing, the section is the normal section, otherwise, it is negative. The forces acting on the negative cross section of point P from the adjacent section is $-\boldsymbol{F}$, and the principal moment is $-\boldsymbol{M}$. Those acting on the normal section are $(\boldsymbol{F} + \Delta\boldsymbol{F})$ and $(\boldsymbol{M} + \Delta\boldsymbol{M})$, respectively.

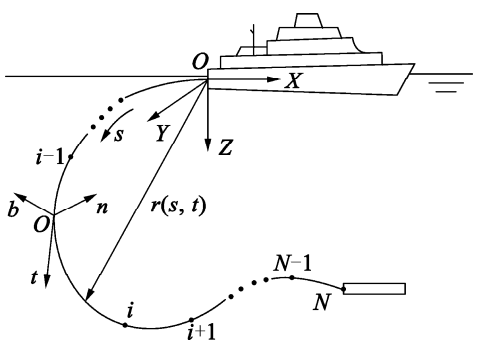

Fig. 1. Sketch of the mooring system.

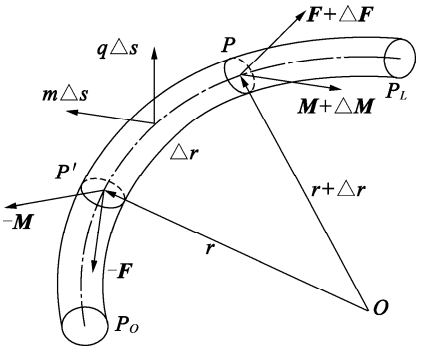

Fig. 2. Infinitesimal element force analysis.

The vector dynamic equation is obtained by applying Newton's second law of motion to the cable-array system element of infinitesimal stretched length ds, as illustrated in Fig. 2.

$$\boldsymbol{F}' + \boldsymbol{q} = \left(\frac{1}{4}\pi d^2 \rho_c\right)\ddot{\boldsymbol{r}}. \tag{4}$$

where d and ρ_c are the diameter and the density of the cable, respectively.

The balance of forces at the point of P may be written

$$\boldsymbol{M}' + \boldsymbol{r}' \times \boldsymbol{F} + \boldsymbol{m} = 0, \tag{5}$$

where $\boldsymbol{q}$ is the vector of applied forces per unit length, and $\boldsymbol{m}$ represents the applied moment per unit length.

For cable with equal principal stiffness, the bending moment is proportional to curvature and is directed along the bi-normal. The resultant moment $\boldsymbol{M}$ can be written as:

$$\boldsymbol{M} = EIk\boldsymbol{b} + GJ\tau\boldsymbol{t}\,, \tag{6}$$

where E is the elasticity modulus, I is the moment of inertia of cross section, k is the curvature, G is the shear modulus, J is the polar moment of inertia of cross section, α is the torsion deformation, and τ is the overall twist of the cable at the point.

$$\tau = \gamma + \alpha'\,. \tag{7}$$

The vector of applied forces per unit length consists of the distributed weight, buoyancy, and hydrodynamic force, which is defined using Morison's well-known approximation.

$$\boldsymbol{w} = (\rho_{\mathrm{c}} - \rho_{\mathrm{w}})\frac{\pi d^2}{4}\boldsymbol{g}\,; \tag{8}$$

$$\boldsymbol{f} = -\boldsymbol{D}\boldsymbol{M}_{\mathrm{A}}\boldsymbol{D}^{\mathrm{T}}\ddot{\boldsymbol{r}}\,; \tag{9}$$

$$\boldsymbol{h} = -\frac{1}{2}\rho_{\mathrm{w}} d\left(\boldsymbol{D}\begin{bmatrix} f_{\mathrm{p}}\boldsymbol{u}\,|\boldsymbol{u}| \\ f_{\mathrm{p}}\boldsymbol{v}\,|\boldsymbol{v}| \\ f_{\mathrm{q}}\boldsymbol{w}\,|\boldsymbol{w}| \end{bmatrix}\right), \tag{10}$$

where ρ_{w} is the density of sea water, $\boldsymbol{M}_{\mathrm{A}}$ is the additional mass matrix, f_{p} is the normal drag coefficient of water on cable, and f_{q} is the tangential drag coefficient of water on cable.

Substituting Eq. (6) into Eq. (5) yields

$$\boldsymbol{t}\times[(EIk\boldsymbol{n})' - GJ\tau k\boldsymbol{b} + \boldsymbol{F}] + (GJ\tau)'\boldsymbol{t} + \boldsymbol{m} = 0\,. \tag{11}$$

The scalar product of Eq. (11) with $\boldsymbol{t}$ yields

$$(GJ\tau)' + \boldsymbol{m}\cdot\boldsymbol{t} = 0\,. \tag{12}$$

If there is no distributed torsion moment (Garret, 1982), it follows from Eq. (12) that the torque $(GJ\tau)$ is independent of arc length s. In the following, both $(GJ\tau)$ and $\boldsymbol{m}$ are assumed to be zero, so that Eq. (11) becomes

$$\boldsymbol{F} = \boldsymbol{T}\cdot\boldsymbol{t} - EIk'\cdot\boldsymbol{n} - EIk\cdot\gamma\cdot\boldsymbol{b} + GJ\tau\cdot k\cdot\boldsymbol{b}\,. \tag{13}$$

where $\boldsymbol{T}$ is the axial tension.

Substituting Eq. (13) into Eq. (4) yields

$$-(EI\boldsymbol{r}'')'' + [(\boldsymbol{T} - EIk^2)\boldsymbol{r}']' + [GJ\tau(\boldsymbol{r}'\times\boldsymbol{r}'')]' + \boldsymbol{q} = \left(\frac{1}{4}\pi d^2\rho_{\mathrm{c}} I\right)\ddot{\boldsymbol{r}}\,,\quad (GJ\tau_i)' = 0\,. \tag{14}$$

3. Finite Element Formalization

Because of the tether's geometrically nonlinear profile, the strong nonlinearities are contained in the hydrodynamic term, and the wide range of tether states that can occur during ROV operation, we look to find an approximation to the true solution of the differential equations of Eq. (14) using numerical techniques.

The discrete form of the differential equations of motion is:

$$-(EI\boldsymbol{r}_i'')''+[(\boldsymbol{T}_i-EIk_i^2)\boldsymbol{r}_i']'+[GJ\tau_i(\boldsymbol{r}_i'\times\boldsymbol{r}_i'')]'+\boldsymbol{q}_i=\boldsymbol{M}_i\ddot{\boldsymbol{r}}_i(GJ\tau_i)'=0\,, \tag{15}$$

where $\boldsymbol{M}_i$ represent the quality of cables, including the added mass aroused by the movement of cable.

To develop the element formulation, we consider a single element of length L and approximate $r(s, t)$ and α by twisted cubic spline (Howard and Syck, 1992) and a linearly varying quantity (Logan, 1993; Rao, 1989)

$$\boldsymbol{r}(s,t): s\in[s^{(i-1)},s^{(i)}]\approx\boldsymbol{r}_i=\sum_{j=1}^{p+1}\sigma_{i,j}(t)\phi_{i,j}(s)\qquad j=1,2,3,4\,; \tag{16}$$

$$\alpha_i=\alpha^{(i-1)}\frac{s^i-s}{s^i-s^{i-1}}+\alpha^{(i)}\frac{s-s^{i-1}}{s^i-s^{i-1}}\,. \tag{17}$$

Take $\delta\boldsymbol{r}_i$ as the weighted function for $\boldsymbol{r}(s,t)$

$$\delta\boldsymbol{r}_i=\delta\phi_{i,j}(s)\,. \tag{18}$$

Using Eq. (16) and Eq. (17), Eq. (15) may be reduced to ordinary differential equations by the Galerkin's method of weighted residuals.

$$\int_{s^{(i-1)}}^{s^{(i)}}\left\{EI\boldsymbol{r}_i'''-\left[(\boldsymbol{T}-EIk^2)_i\boldsymbol{r}_i'\right]-\left[GJ\tau_i(\boldsymbol{r}_i'\times\boldsymbol{r}_i'')\right]\phi_{i,j}'+\left[\boldsymbol{q}_i-\left(\frac{1}{4}\pi d^2\rho I\right)\ddot{\boldsymbol{r}}_i\right]\phi_{i,j}\right\}\mathrm{d}s$$

$$=\left\{\left\{EI\boldsymbol{r}_i'''-(\boldsymbol{T}-EIk^2)_i\boldsymbol{r}'-[GJ\tau_i(\boldsymbol{r}_i'\times\boldsymbol{r}_i'')]\right\}\phi_{i,j}\right\}\Big|_{s^{(i-1)}}^{s^{(i)}}\qquad j=1,2,3,4 \tag{19}$$

$$GJ\int_{s^{(i-1)}}^{s^{(i)}}(\gamma_i+\alpha_i')\phi_{i,j}'\mathrm{d}s=[GJ\tau_i]\phi_{i,j}\Big|_{s^{(i-1)}}^{s^{(i)}}\qquad j=1,3 \tag{20}$$

The equations of motion in Eq. (19) for an element may be written as:

$$(\boldsymbol{K}_{\mathrm{B}i}+\boldsymbol{K}_{\mathrm{A}i}+\boldsymbol{K}_{\tau i})\boldsymbol{X}_i+\boldsymbol{M}_{\mathrm{e}i}\ddot{\boldsymbol{X}}_i+\boldsymbol{q}_i=0 \tag{21}$$

where the 12×12 system matrices $\boldsymbol{K}_{\mathrm{B}i}$, $\boldsymbol{K}_{\mathrm{A}i}$ and $\boldsymbol{K}_{\tau i}$ embody generalized bending, axial, and torsion forces, respectively, that are applied at the element nodes and resulted from the curvature, axial strain, and twist experienced throughout the cable element; $\boldsymbol{M}_{\mathrm{e}i}$ is the element mass matrix of the cable; $\boldsymbol{q}_i=\boldsymbol{W}_i+\boldsymbol{H}_i+\boldsymbol{B}_i$, where the generalized load vectors $\boldsymbol{W}_i$, $\boldsymbol{H}_i$, and $\boldsymbol{B}_i$ define the weight and buoyancy, hydrodynamic, and boundary forces, respectively; and the 12×1 vector, $\boldsymbol{X}_i=\{\boldsymbol{r}_i^{(i-1)\mathrm{T}}\ \boldsymbol{r}_i''^{(i-1)\mathrm{T}}\ \boldsymbol{r}_i^{(i)\mathrm{T}}\ \boldsymbol{r}_i''^{(i)\mathrm{T}}\}^{\mathrm{T}}$.

$$\boldsymbol{K}_{\mathrm{B}i}=\int_0^l EI\boldsymbol{r}_i'''\phi_{i,j}'\,\mathrm{d}s\qquad j=1,\,2,\,3,\,4\,; \tag{22}$$

$$\boldsymbol{K}_{\mathrm{A}i}=\int_0^l\lambda_i\boldsymbol{r}_i'\phi_{i,j}'\,\mathrm{d}s\qquad j=1,\,2,\,3,\,4\,; \tag{23}$$

$$\boldsymbol{K}_{\tau i}=\int_0^l GJ\tau_i(\boldsymbol{r}_i'\times\boldsymbol{r}_i'')\phi_{i,j}'\,\mathrm{d}s\qquad j=1,\,2,\,3,\,4\,; \tag{24}$$

$$\boldsymbol{M}_{\mathrm{e}i}=\int_0^l(\boldsymbol{M}_i)\phi_{i,j}\,\mathrm{d}s\qquad j=1,\,2,\,3,\,4\,; \tag{25}$$

$$\boldsymbol{q}_i=\int_0^l(\boldsymbol{w}+\boldsymbol{f}+\boldsymbol{h})\phi_{i,j}\,\mathrm{d}s\qquad j=1,\,2,\,3,\,4\,. \tag{26}$$

λ_i can be written as:

$$\lambda_i = T_i - EI(\boldsymbol{r}'' \cdot \boldsymbol{r}'')^{i-1/2}, \tag{27}$$

where T_i is the elastic force in the element.

Eq. (20) may be written as:

$$\frac{GJ}{L_i}\begin{bmatrix} 1 & -1 \\ -1 & 1 \end{bmatrix}\begin{Bmatrix} \alpha_{i-1} \\ \alpha_i \end{Bmatrix} = GJ\begin{Bmatrix} \gamma_i \\ -\gamma_i \end{Bmatrix} + \begin{Bmatrix} -GJ\tau_i^{i-1} \\ GJ\tau_i^i \end{Bmatrix} \tag{28}$$

where, the boundary terms $GJ\tau_i^{i-1}$ and $GJ\tau_i^i$ represent the internal restoring torque at the boundaries of the element.

To create the overall equation of motion, we concatenate a series of the twisted cubic spline elements. This process, referred to as assembly, is represented mathematically by the application of Eq. (21) for i=1, 2, …, N. This assembly process forms the global system of motion equations (Fang *et al*., 2009):

$$\left\{\boldsymbol{K}_{\mathrm{BG}} + \boldsymbol{K}_{\mathrm{AG}} + \boldsymbol{K}_{\tau\mathrm{G}}\right\}\left\{\boldsymbol{r}_0^{\mathrm{T}}\boldsymbol{r}_0''^{\mathrm{T}}\boldsymbol{r}_1^{\mathrm{T}}\boldsymbol{r}_1''^{\mathrm{T}}\cdots\boldsymbol{r}_N^{\mathrm{T}}\boldsymbol{r}_N''^{\mathrm{T}}\right\}^{\mathrm{T}} + \boldsymbol{H}_{\mathrm{G}} + \boldsymbol{W}_{\mathrm{G}} + \boldsymbol{B}_{\mathrm{G}} = \boldsymbol{M}_{\mathrm{G}}\ddot{\boldsymbol{D}}, \tag{29}$$

where $\boldsymbol{K}_{\mathrm{BG}}$, $\boldsymbol{K}_{\mathrm{AG}}$ and $\boldsymbol{K}_{\tau G}$ are the global bending, axial, and torsion stiffness matrices, respectively; $\boldsymbol{H}_{\mathrm{G}}$ is the global vector of hydrodynamic forces acting on the node points of the assembled model; $\boldsymbol{W}_{\mathrm{G}}$ is the assembly of weight and buoyancy forces; $\boldsymbol{B}_{\mathrm{G}}$ defines the boundary loads applied over the assembled tether; and $\boldsymbol{M}_{\mathrm{G}}$ is the total mass matrix of the cable.

In addition to the global system of motion equations, the torsion constraint equations given by Eq. (20) are assembled to produce a global system of constraint equations that define the torsion deformation throughout the tether:

$$GJ\begin{bmatrix} \frac{1}{L_1} & -\frac{1}{L_1} & 0 & 0 & 0 \\ -\frac{1}{L_1} & \frac{1}{L_1}+\frac{1}{L_2} & -\frac{1}{L_2} & 0 & 0 \\ 0 & \ddots & \ddots & \ddots & 0 \\ 0 & 0 & -\frac{1}{L_{N-1}} & \frac{1}{L_{N-1}}+\frac{1}{L_N} & -\frac{1}{L_N} \\ 0 & 0 & 0 & -\frac{1}{L_N} & \frac{1}{L_N} \end{bmatrix}\begin{Bmatrix} \alpha_0 \\ \alpha_1 \\ \vdots \\ \alpha_{N-1} \\ \alpha_N \end{Bmatrix} = GJ\begin{Bmatrix} \gamma_1 \\ \gamma_2-\gamma_1 \\ \vdots \\ \gamma_N-\gamma_{N-1} \\ -\gamma_N \end{Bmatrix} + \begin{Bmatrix} T_0 \\ 0 \\ 0 \\ 0 \\ T_N \end{Bmatrix} \tag{30}$$

In order to enforce smoothness and continuity of the twisted spline elements across the node points, the curvature vectors at the nodes must satisfy a series of constraint equations defined over the scope of the concatenated twisted spline elements. For a cable with N elements that are concatenated to extend between nodes 0 and N, these constraint equations (Press *et al.*, 1992) take the form:

$$\begin{bmatrix} \frac{L_1}{3}\boldsymbol{I} & \frac{L_1}{6}\boldsymbol{I} & \boldsymbol{0} & \boldsymbol{0} & \boldsymbol{0} \\ \frac{L_1}{6}\boldsymbol{I} & \frac{L_1+L_2}{3}\boldsymbol{I} & \frac{L_2}{6}\boldsymbol{I} & \boldsymbol{0} & \boldsymbol{0} \\ \boldsymbol{0} & \ddots & \ddots & \ddots & \boldsymbol{0} \\ \boldsymbol{0} & \boldsymbol{0} & \frac{L_{N-1}}{6}\boldsymbol{I} & \frac{L_{N-1}+L_N}{3}\boldsymbol{I} & \frac{L_N}{6}\boldsymbol{I} \\ \boldsymbol{0} & \boldsymbol{0} & \boldsymbol{0} & \frac{L_N}{6}\boldsymbol{I} & \frac{L_N}{3}\boldsymbol{I} \end{bmatrix} \begin{bmatrix} \boldsymbol{r}_0'' \\ \boldsymbol{r}_1'' \\ \vdots \\ \boldsymbol{r}_{N-1}'' \\ \boldsymbol{r}_N'' \end{bmatrix} = \begin{bmatrix} \frac{\boldsymbol{r}_1-\boldsymbol{r}_0}{L_1} \\ \frac{\boldsymbol{r}_2-\boldsymbol{r}_1}{L_2}-\frac{\boldsymbol{r}_1-\boldsymbol{r}_0}{L_1} \\ \vdots \\ \frac{\boldsymbol{r}_N-\boldsymbol{r}_{N-1}}{L_N}-\frac{\boldsymbol{r}_{N-1}-\boldsymbol{r}_{N-2}}{L_{N-1}} \\ -\frac{\boldsymbol{r}_N-\boldsymbol{r}_{N-1}}{L_N} \end{bmatrix} + \begin{bmatrix} -\boldsymbol{r}_0' \\ 0 \\ \vdots \\ 0 \\ \boldsymbol{r}_N' \end{bmatrix} \tag{31}$$

4. Solution Procedure

Recalling that the node curvatures are an explicit function of the node positions, the left-hand side of Eq. (21) is seen to be an explicit function of the node positions and, through the hydrodynamic terms, node velocities. The series of global motion equations in Eq. (21) thus forms a series of 3(N+1) second-order differential equations of the form

$$\boldsymbol{F}(\boldsymbol{D},\dot{\boldsymbol{D}}) = \boldsymbol{M}_{\mathrm{G}}\ddot{\boldsymbol{D}} . \tag{32}$$

Consider the dynamic response of rope in the three dimensional space, Eq. (32) can be treated as a series of first-order equations and calculated by the method of Runge-Kutta. Thus, give an initial state of the tether, $\boldsymbol{Y}(t_0) = \left\{\boldsymbol{r}_0^{\mathrm{T}}(t_0)\ \dot{\boldsymbol{r}}_0^{\mathrm{T}}(t_0)\ \boldsymbol{r}_1^{\mathrm{T}}(t_0)\ \cdots\ \boldsymbol{r}_N^{\mathrm{T}}(t_0)\ \dot{\boldsymbol{r}}_N^{\mathrm{T}}(t_0)\right\}$. The entire solution process is to calculate $\boldsymbol{Y}(t_1)$, $\boldsymbol{Y}(t_2)$, $\boldsymbol{Y}(t_3)$,⋯, $\boldsymbol{Y}(t_k)$, $\boldsymbol{Y}(t_{k+1})$, $\boldsymbol{Y}(t_f)$, and t_f is the duration of the simulation. The procedure of calculations from the k-th step to the (k+1)-th step following the sequence is shown in Fig. 3.

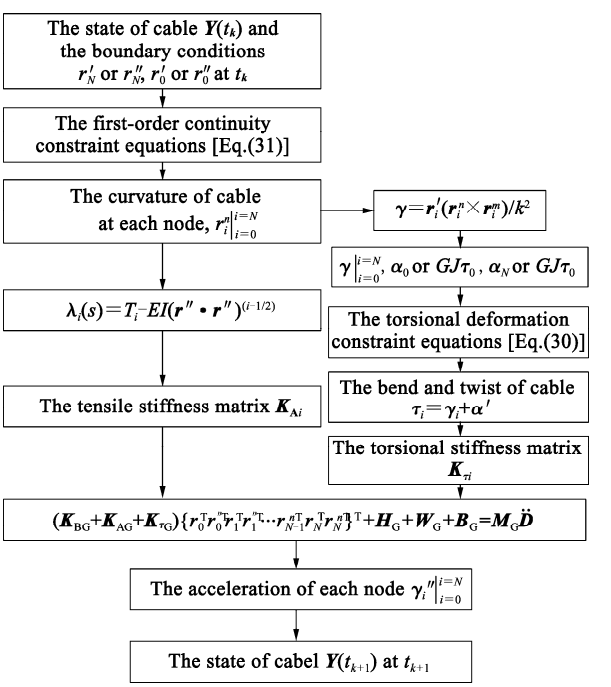

Fig. 3. Flow chart of the calculation.

5. Numerical Application

In this paper, the mode is used for an existing experiment to verify its correctness. The initial state is that the cable suspends in the sink, and the velocity of water is 3 kn. The weight of objects hanging at the cable is 8.9 N, the length of the cable is 3.66 m, the diameter of the cable is 3.05 mm, and the simulation time is 12 s. According to Fig. 4, the cable gets to its steady state from 8 s, which is consistent with the experimental results (Zhu *et al*., 2002).

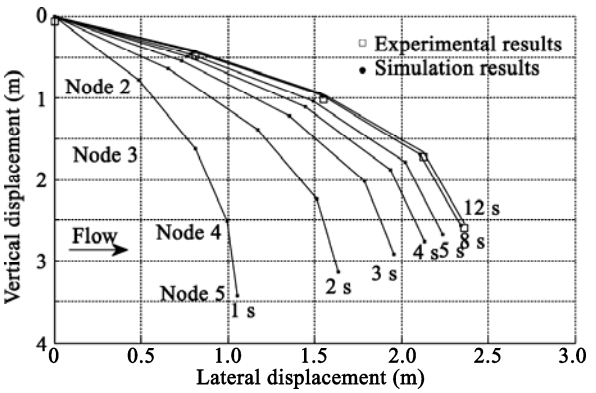

Fig. 4. Comparison of the modeling results with the test results.

Based on the cable model previously discussed, the model is used for the cable releasing and recycling by increasing the number of node and changing the first element length. Get the changes of the shape and tension of cable in the process of releasing the cable.

The whole process is as follows: the initial length of the cable is 60 m, stationary vertical downward. The weight of objects hanging at the cable is 1200 N and its hydraulic resistance is 1025 N. The ship speeds up from 0 to 5 s, and then keeps the preset speed until 360 s. The cable is relaxed from 0 to 1 m/s during 2 s, and then keeps the speed of 1 m/s until 420 s. Followed by 2 s, the speed of relaxing cable slows down to zero. At this time, the length cable reaches 120 m, and then it will keep moving at the preset velocity. In this paper, we analyze the movement of cable when the speed is 1.543 and 3.086 m/s.

Fig. 5 shows the change of cable-shape during the process of the drag by the velocity of 1.543 m/s. The depth-time curves of towed vehicle are shown in Fig. 6. We can obtain that when the drag speed is larger, the change of depth is smaller at the same relax length, which is consistent with the experimental results.

Fig. 7 shows the tension-time curves. The larger the drag speed, the larger the tension. Beside, the tension has large changes when the speed of the relax cable increases or decreases. The tension of the cable increases steadily when the relaxing speed of cable is constant.

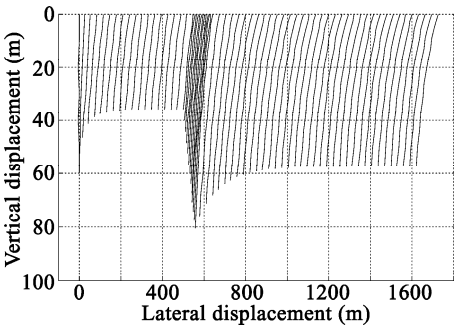

Fig. 5. Change of cable-shaped with time.

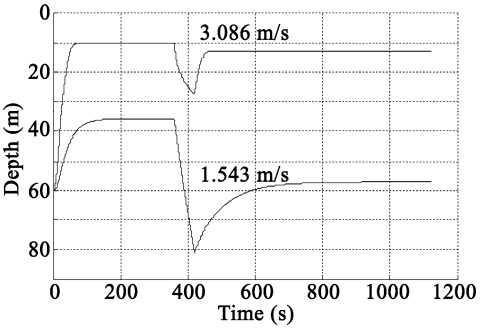

Fig. 6. Depth change of towed vehicle with time.

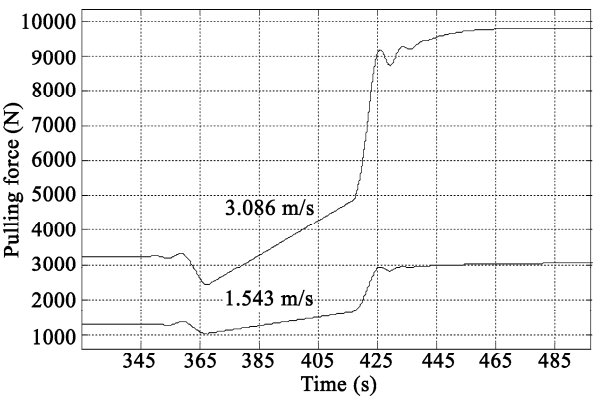

Fig. 7. Tension change of cable during the process of cable relaxing.

6. Conclusion

A finite element model for low tension cable in the towed system is developed and implemented. The cable model is represented by the discretized motion equations by using a weighted residual approach that treats the cubic spline interpolation function as the trial solution. Compared with the existing finite element models, the model has less number of variables and maintains the advantages of simpler linear finite element approaches. This work captures the dynamics characteristic of low-tension cable in three dimensions correctly and stably, and thus makes it suitable for solving a series of undersea cable dynamics problems.

References

Ablow, C. M. and Schechter, S., 1983. Numerical simulation of under sea cable dynamics, *Ocean Eng*., **10**(6): 443–457.

Banerjee, A. K. and Do, V. N., 1994. Deployment control of a cable connecting a ship to an underwater vehicle, *J. Guid. Control Dyn*., **17**(4): 1327–1332.

Buckham, B., Frederick, R. D. and Nahon, M., 2004. Development of a finite element cable model for use in low-tension dynamics simulation, *J. Appl. Mech.*, **71**(4): 476–485.

Burgess, J. J., 1992. Equations of motion of a submerged cable with bending stiffness, *Proc. 11th Int. Conf. Offshore Mech. Arctic Eng.* (*OMAE*), Calgary, Canada, Vol. 1, Pt A: 283–289.

Dowling, A. P., 1988. The dynamics of towed flexible cylinders, Part 1. Neutrally buoyant elements, *J. Fluid Mech*., **187**, 507–532.

Fang, Z. F., He, Q. S., Xiao, H. P. and He, K. D., 2012. *Finite Element Computer Program for Underwater Cable*, National Copyright Administration of the People's Republic of China, 2012SR049491. (in Chinese)

Fang, Z. F., Wu, J. H., He, K. D. and Zhang, M. S., 2009. The impact dynamic model of steel cables, *Engineering Mechanics*, **26**(10): 197–202. (in Chinese)

Garret, D. L., 1982. Dynamic analysis of slender rods, *J. Energy Resour. Technol*., **104**(4): 302–306.

Grosenbaugh, M. A., Howell, C. T. and Moxnes, S., 1993. Simulating the dynamics of underwater vehicle with low-tension tethers, *Int. J. Offshore Polar Eng.*, **3**(3): 213–218.

Howard, B. E., and Syck, J. M., 1992. Calculation of the shape of a towed underwater acoustic array, *IEEE J. Ocean. Eng*., **17**(2): 193–201.

Howell, C. T., 1991. Numerical analysis of 2-D nonlinear cable equations with applications to low-tension problems, *Proc. 1st Offshore Polar Eng. Conf.* (*ISOPE*), Edinburgh, UK, Vol.2, 203–209.

Logan, D. L., 1993. *A First Course in the Finite Element Method*, 2nd Ed, PWS, Boston, MA, 195–239.

Park, H. I., Jung, H. and Koterayama, W., 2003. A numerical and experimental study on dynamics of a towed low-tension cable, *Appl. Ocean Res.*, **25**(5): 289–299.

Press, W. H., Teukolsky, S. A., Vetterling, W. T. and Flannetry, B. P., 1992. *Numerical Recipes in C*, Cambridge University Press, New York, 113–117.

Rao, S. S., 1989. *The Finite Element Method in Engineering*, 2nd Ed, Pergamon Press, Toronto, 101–198, 291–300.

Sun, Y., Leonard, J. W. and Chiou, R. B., 1994. Simulation of unsteady oceanic cable deployment by direct integration with suppression, *Ocean Eng*., **21**(3): 243–256.

Triantafyllou, M. S., 1984. The dynamics of taut inclined cables, *Quarterly Journal of Mechanics and Applied Mathematics*, **37**(3): 421–440.

Zhu, J., Li, W. and Cheng, H., 2006. Numerical simulation of nonlinear dynamic movement of towed cable-ship, *The Ocean Engineering*, **24**(3): 56–62. (in Chinese)

Zhu, K. Q., Li, D. G. and Li, W. Y., 2002. Lumped- parameter analysis method for time-domain of ocean cable-body systems, *The Ocean Engineering*, **20**(2): 100–102. (in Chinese)

Zhu, K. Q., Zheng, D. C., Zhang, Y. S., Yu, C. L., Wang, R., Shu, H. P., Zhao, Z. P., Ma, X. F. and Zhang, C. H., 2010. A study on the strong nonlinear coupling space movement of underwater tethed remotely operated vehicle & sling safety under irregular waves, *The Ocean Engineering*, **28**(2): 95–99. (in Chinese)

Zhu, K. Q., Zhu, H. Y., Yu, C. L., Ma, X. F., Zhang, R. S., Zheng, D. C. and Gao, J., 2008. Simulation of nonlinear coupling dynamic characteristic on a deep-sea tethered remotely operated vehicle multi-body system, *The Ocean Engineering*, **26**(1): 83–87. (in Chinese)